HHS Public Access

Author manuscript

Cell Rep. Author manuscript; available in PMC 2016 December 01.

Published in final edited form as:

Cell Rep. 2016 November 15; 17(8): 2028–2041. doi:10.1016/j.celrep.2016.10.068.

Pancreatic Inflammation Redirects Acinar to Beta Cell Reprogramming

Hannah W. Clayton[1,2], **Anna B. Osipovich**[2,3], **Jennifer S. Stancill**[1,2], **Judsen D. Schneider**[2], **Pedro G. Vianna**[2], **Carolyn M. Shanks**[2], **Weiping Yuan**[2], **Guoqiang Gu**[1,2], **Elisabetta Manduchi**[4], **Christian J. Stoeckert Jr.**[4], and **Mark A. Magnuson**[1,2,3,*]

[1]Department of Cell and Developmental Biology, Vanderbilt University, Nashville, TN, 37232, USA

[2]Center for Stem Cell Biology, Vanderbilt University, Nashville, TN, 37232, USA

[3]Department of Molecular Physiology and Biophysics, Vanderbilt University, Nashville, TN, 37232, USA

[4]Institute for Biomedical Informatics and Department of Genetics, University of Pennsylvania School of Medicine, Philadelphia, PA, 19104, USA

Summary

Using a transgenic mouse model to express *MafA*, *Pdx1,* and *Neurog3* (3TF) in a pancreatic acinar cell- and doxycycline-dependent manner, we discovered that the outcome of transcription factor-mediated acinar to β-like cellular reprogramming is dependent on both the magnitude of 3TF expression and on reprogramming-induced inflammation. Overly robust 3TF expression causes acinar cell necrosis resulting in marked inflammation and acinar-to-ductal metaplasia. Generation of new β-like cells requires limiting reprogramming-induced inflammation, either by reducing 3TF expression or by eliminating macrophages. The new β-like cells were able to reverse streptozotocin-induced diabetes 6 days after inducing 3TF expression but failed to sustain their function after removal of the reprogramming factors.

Graphical Abstract

*Corresponding author: mark.magnuson@vanderbilt.edu.

Accession number

The accession number for the RNASeq data at ArrayExpress is E-MTAB-3921.

Author Contributions

Conceptualization, H.W.C., A.O., and M.A.M.; Methodology, H.W.C., A.O., J.D.S., W.Y., and E.M.; RNA-seq Analyses, E.M. and C.J.S.; Investigation, H.W.C., C.S., J.D.S., P.G.V., J.S.S., and W.Y.; Resources, G.G.; Writing-Original draft, H.W.C. and M.A.M.; Writing-Review & Editing, A.O., H.W.C, and M.A.M; Visualization, H.W.C., A.O., M.A.M, and C.J.S.; Project Administration, H.W.C. and M.A.M; Funding Acquisition, M.A.M.

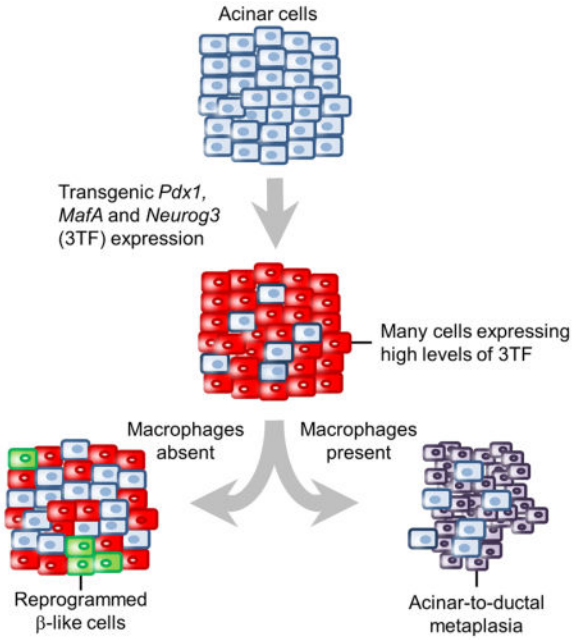

Introduction

Reprogramming of pancreatic cells into new β-like cells represents a potential therapy for Type 1 diabetes (Bramswig et al., 2013; Dor et al., 2004; Li et al., 2014c; Thorel et al., 2010; Zhou et al., 2008). Pancreatic acinar cells are an appealing target for cellular reprogramming since they are abundant, derived from a common progenitor cell during pancreatic organogenesis (Gu et al., 2002), and exhibit significant transcriptional plasticity (Li et al., 2014c; Puri et al., 2015; Ziv et al., 2013). Towards this end, Zhou et al. reported that adenoviral-mediated expression of three pancreas-specific transcription factors *MafA, Pdx1,* and *Neurog3* (3TF) in immunocompromised *Rag1*$^{-/-}$ mice results in the conversion of pancreatic acinar cells into new insulin-secreting β-like cells (Zhou et al., 2008). In addition, transient administration of epidermal growth factor and ciliary neurotrophic factor has also been reported to convert pancreatic acinar cells into new β-like cells (Baeyens et al., 2013).

While the reports of acinar to β-cell (A→β) reprogramming appear promising, the effects of reprogramming on the microscopic anatomy, cellular function, and physiological function of the pancreas have not been explored but would be expected to be substantial due to the very marked physiological and histological differences between acinar and β-cells. In contrast to pancreatic β-cells, acinar cells produce copious amounts of proteases, lipases, and ribonucleases whose potentially auto-digestive abilities require sequestration mechanisms to prevent endogenous tissue damage (Logsdon and Ji, 2013). The exocrine pancreas protects itself from autodigestion through several mechanisms. First, many of the enzymes are secreted as inactive pro-enzymes, or zymogens, which only become active within the duodenum (Neurath and Walsh, 1976). Second, the proteolytic enzymes are co-secreted with a trypsin inhibitor that prevents premature activation of trypsinogen, which normally becomes activated in the small intestine and is responsible for activation of the other

precursor digestive enzymes (Logsdon and Ji, 2013). Third, acinar-to-ductal metaplasia (ADM) occurs (Bockman et al., 1997; Liou et al., 2013; Pan et al., 2013) and has been suggested to limit autodigestion in the face of acinar cell injury (Puri et al., 2015).

ADM, the conversion of acinar cells into a non-secretory duct-like cell, is characterized by the formation of duct-like complexes and fibrosis (Wang et al., 1995) in response to pancreatic inflammation. The mechanisms that initiate the inflammation are disputed. Some argue that it is due to intracellular activation of trypsinogen (Halangk et al., 2000; Szilagyi et al., 2001; Van Acker et al., 2002; Whitcomb et al., 1996) whereas others have suggested that it is due to calcium overload (Li et al., 2014a) and endoplasmic reticulum (ER) stress (Ji et al., 2003; Logsdon and Ji, 2013). In either case, ADM is characterized by aberrant expression of cytokeratins (Strobel et al., 2007), *Pdx1*, *Sox9,* and *Onecut1* in pancreatic acinar cells (Rooman and Real, 2012).

In order for an *in vivo* β-cell restorative therapy to become clinically feasible, a better understanding of the factors that modulate intercellular conversions and the physiological effects that such conversions may induce is required. Towards this end, we developed a diallelic transgene-based mouse model that expresses 3TF specifically in pancreatic acinar cells in a tetracycline-dependent manner. Such a model enables 3TF expression to be modulated in a manner that is unachievable using a virus-based expression system, thereby allowing us to examine the effects of both 3TF concentration and duration on generating new β-like cells. Our studies using this model indicate that the level of 3TF expression has a major influence, not only on reprogramming success but also on tissue response. Indeed, we found that robust 3TF expression causes acinar cell stress, marked inflammation, and ADM, and that attenuating reprogramming-induced inflammation, either by reducing 3TF expression or eliminating macrophages, results in the production of new β-like cells. Moreover, the duration of factor expression may also play a role in the reprogramming outcome since the ability of new β-like cells to improve glycemia was dependent on the dox-induced expression of 3TF, with removal of dox resulting in a worsening of glycemic control and reversion to a fully diabetic state within a few days.

Results

Design and validation of mouse alleles

To explore the cellular dynamics of pancreatic A→β reprogramming, we developed a diallelic transgene-based mouse model that co-expresses both 3TF and mCherry specifically in pancreatic acinar cells in a tetracycline-inducible manner (Figure 1A). The first allele (*Rosa26*$^{3TF.mCherry}$) was made by replacing the coding sequences for *Ptf1a* with those for the reverse tetracycline Trans-Activator (rtTA). In the second allele (*Ptf1a*^{rtTA}), a bi-directional Tet-operator cassette that in one direction expresses a 2A peptide-linked fusion gene of *MafA*, *Pdx1,* and *Neurog3* and in the other direction the red fluorescent protein *mCherry* was inserted into a functionally disabled *Rosa26/SetD5* gene locus (Chen et al., 2011). When adult mice containing both the *Ptf1a*^{rtTA} and *Rosa26*$^{3TF.mCherry}$ alleles were given 2.0 mg/ml doxycycline (dox) in their drinking water for 1 day, red fluorescence was observed in the pancreas but no other visceral organs (Figure 1B). Furthermore, mCherry expression in the pancreas was restricted to acinar cells and not observed in pancreatic ducts

or endocrine cells, as expected due to the acinar cell-restricted expression of *Ptf1a* at this age (Figure 1C, S1A). Immunofluorescent staining for both mCherry and amylase indicated that 78% (±2.5%; n=3) of acinar cells expressed mCherry. Staining for mCherry and for each of the reprogramming factors showed that virtually all mCherry-positive ($^+$) cells expressed the reprogramming factors (Figure 1D).

To further validate the experimental model, we analyzed the function of the 2A peptide-cleaved transcription factors generated by the *Rosa26*$^{3TF.mCherry}$ allele. First, immunoblot analysis showed PDX1, which is flanked by MAFA and NEUROG3 protein sequences in the 2A peptide-containing cassette, to be properly cleaved from the two surrounding proteins (Figure 1E). Second, analysis of protein function using reporter genes showed that each of the 2A peptide-modified proteins functioned in a normal manner, indistinguishable from that of their wild-type counterparts (Figure S1B–E). Third, a recombinant adenovirus containing the 3TF fusion gene, when injected together with a GFP-expressing virus into the pancreas of *Rag1*$^{-/-}$ mice, resulted in scattered insulin$^+$/GFP$^+$ co-expressing cells within the exocrine compartment of the pancreas, similar to those observed by Zhou et al. (Zhou et al., 2008) (Figure S1F, G). Together, these findings confirmed that the 2A peptide-modified MAFA, PDX1, and NEUROG3 made in response to dox-induction functioned normally.

Lack of A→β reprogramming in transgenic mice after 3TF induction

Since viral mediated expression of 3TF in the pancreas has previously been reported to cause A→β conversion in 10 days or less (Zhou et al., 2008), we treated our diallelic mice with dox for 1, 7, and 28 days and performed immunostaining for acinar and endocrine cell markers, including insulin. At 1 day, the 3TF-induced cells resembled acinar cells with all mCherry$^+$ cells seen to express amylase, an acinar cell-specific marker. However, at 7 and 28 days, the expression of amylase in mCherry$^+$ cells was greatly diminished or absent (Figure 2A, B). In addition, the mCherry$^+$ cells were smaller and located in tubular-like cell clusters (Figure 2A). Chromogranin A, an endocrine cell marker that was absent in the 1 day sample, was expressed in nearly 100% of mCherry$^+$ cells at 7 and 28 days (Figure 2A, B). Interestingly, despite the widespread expression of this endocrine marker in mCherry$^+$ cells, we failed to observe any insulin, glucagon, somatostatin, or pancreatic polypeptide expression by immunofluorescence staining. However, after 7 days of dox treatment, we did observe that approximately 40% of mCherry$^+$ cells expressed ghrelin, a hormone normally expressed in 1% or fewer adult pancreatic endocrine cells (Arnes et al., 2012). The portion of cells expressing ghrelin rose to nearly 60% in the 28 day sample (Figure 2A, B).

RNA profiling of the 3TF-treated cells

To better understand why new β-like cells were not observed and to corroborate the immunostaining results, we performed RNA-Seq on FACS-purified mCherry$^+$ cells after 1 and 7 days of dox administration and compared their transcriptional profiles to FACS-purified uninduced acinar cells (Table S1). These datasets revealed that *MafA, Pdx1,* and *Neurog3* mRNAs were all highly up-regulated after 1 day of dox treatment compared to uninduced acinar cells. Indeed, *MafA* increased from 0.67 ± 0.67 to 4069 ± 169, *Pdx1* from 20 ± 4 to 7037 ± 471, and *Neurog3* from 0 to 10931 ± 629 normalized counts (Table S1), strongly suggesting that the lack of insulin gene expression was not due to insufficient 3TF

expression. Furthermore, inspection of the 7 day 3TF-induced RNA-seq dataset showed that while some genes that characterize either immature or mature β-cells, such as *ChgA, Ghrl, Neurod1,* and *Insm1,* were highly up-regulated compared to uninduced acinar cells, other genes that are normally present in β-cells such as *Ins1*, *Ins2*, *Nkx6.1*, *Isl1*, and *Pax6* were not identified as significantly up-regulated in the 3TF-induced acinar cells (Figure S2A and Table S2, S3). In addition, many of the endocrine-specific genes that were up-regulated have been previously shown to be direct DNA binding targets for either *Neurog3, Pdx1,* or *MafA*. For instance, *Neurod1*, *Nkx2.2,* and *Insm1* are targets of *Neurog3* (Huang et al., 2000; Smith et al., 2003; Watada et al., 2003) and *Pdx1* binds to the promoters of both *Gck* and *Slc2a2* (Khoo et al., 2012; Watada et al., 1996). Importantly, we also noticed that many of the upregulated genes from the RNA-seq data set of 7 day dox-induced acinar cells were associated with inflammation (Figure S2B). Taken together, these findings suggest that while 3TF expression increased expression of several endocrine-specific genes, it did not cause acinar cells to thoroughly adopt a β-cell-like gene expression profile.

Transgene-based expression of 3TF results in acinar-to-ductal metaplasia

To confirm that inflammation-associated genes were expressed in response to 3TF-induction, we stained pancreata for inflammatory cells using CD45, a pan-leukocyte marker, and observed that nearly a third of the cells present in the pancreas were leukocytes (Figure 3A, B). Staining for F4/80, a macrophage marker, and CD3, a T-cell marker, revealed that both inflammatory cells were present with the majority being macrophages (Figure S3A, B). Finally, Masson's trichrome staining revealed extensive fibrosis further indicating a potent inflammatory response (Figure S3C).

Since pancreatic inflammation has been linked to metaplastic changes, we examined the histological appearance of 7 day-induced pancreatic tissue. After 7 days of 3TF expression, pancreata of the diallelic mice were smaller (Figure 3C) and characterized by the presence of many tubular complexes (Figure 3D), all of which are hallmarks of ADM (Jura et al., 2005; Parsa et al., 1985). Immunostaining for cytokeratin, a marker for pancreatic duct cells, further revealed that the 3TF-expressing $mCherry^{+}$ cells had adopted duct-like characteristics (Figure 3E, F). After 2 days of dox, and prior to the onset of ADM, we observed acinar cell necrosis (Figure S3D). Since marked inflammation and metaplasia was not observed in our viral control experiments (Figure S1H, I) or previously reported by others when an adenovirus was used to introduce 3TF to the pancreas of normoglycemic mice (Cavelti-Weder et al., 2016; Zhou et al., 2008), we hypothesized that the overly robust 3TF expression that occurred using 2.0 mg/ml of dox was responsible for both the immune response and metaplastic changes.

To determine why 3TF expression in our diallelic transgenic model was causing pancreatic inflammation, we considered the fact that pancreatic acinar cells are especially vulnerable to ER dysfunction owing to their high level of protein synthetic and secretory activity (Ji et al., 2003; Logsdon and Ji, 2013). In support of this notion, we noticed that 44 of 83 genes involved in the activation of the unfolded protein response (UPR) were upregulated after 7 days of 3TF expression (Figure S3E). In addition, expression of genes encoding voltage-gated and other Ca^{2+} channels (Table S4) were also markedly increased. In acinar cells, a

rise in $[Ca^{2+}]_i$ has been associated with ADM and is known to cause activation of inflammatory genes and the ER stress response (Sah et al., 2014). These findings are consistent with activation of the ER stress response in 3TF-expressing acinar cells, possibly by disrupting intracellular calcium homeostasis.

Rag1 or adenovirus infection does not alter the reprogramming outcome

Given that new β-like cells were observed only when 3TF was expressed by an adenoviral vector, but not from a transgene, we performed several experiments to exclude a role for two experimental variables that might have accounted for this divergent reprogramming outcome. The first experimental variable was the presence or absence of *Rag1* (Zhou et al., 2008), a gene required for V(D)J recombination in B and T cells. *Rag1* null mice were used in the adenoviral expression studies to prevent clearance of transcription factor-expressing viruses whereas the transgene-based expression studies utilized $Rag1^{+/+}$ animals since viral clearance was not an issue. Since it is possible that the lack of mature B and T lymphocytes in $Rag1^{-/-}$ mice might modulate the inflammatory response and allow reprogramming to occur, we crossed the *Rag1* null allele into our diallelic mice to derive $Ptf1a^{rtTA/+}$; $Rosa26^{3TF.mCherry/+}$; $Rag1^{-/-}$ mice, then treated these mice with dox for 7 days. Pancreas immunostaining for CD3 showed that T cells were indeed absent (Figure S4A). However, similar to the $Rag1^{+/+}$ mice, many F4/80$^+$ cells were observed in the pancreas after 7 days of dox treatment (Figure S4B) and many cytokeratin$^+$ tubular complexes were formed (Figure S4C,D) that expressed ghrelin (Figure S4F). Masson's trichrome staining again revealed extensive fibrosis (Figure S4E) and, more importantly, there were no cells that co-expressed mCherry and insulin (Figure S4G). These findings showed that the presence or absence of *Rag1* has no substantive role in determining the reprogramming outcome when we used 2.0 mg/ml dox to induce 3TF expression.

The second experimental variable was adenoviral infection. Since it has been reported that viral infection and the presence of adenoviral regulatory proteins could improve reprogramming efficiency (Lee et al., 2012; Wang et al., 2007; Zaldumbide et al., 2012), we simultaneously induced 3TF expression for 7 days using 2.0 mg/ml dox while also injecting a GFP-expressing adenovirus directly into the pancreas (Figure S5A, B). Once again, and despite examining over 600 mCherry and GFP co-expressing cells, no cells were seen that also expressed insulin (Figure S5D). Instead, many of the mCherry and GFP co-expressing cells continued to express ghrelin (Figure S5C). These findings enabled us to exclude the host immune response to viral infection as having a major role in the divergent reprogramming outcome when using 2.0 mg/ml dox to induce 3TF expression.

Reducing the level of 3TF expression lowers the coinciding immune response promoting A→β reprogramming

Given that transgenic expression of 3TF induced widespread pancreatic inflammation, we next explored the effect of varying 3TF expression by treating the diallelic mice with a 10- and 100-fold lower concentration of dox for 7 days. Both groups of mice exhibited lower levels of mCherry fluorescence, consistent with 3TF expression being reduced (Figure 4A, B). We also observed that fewer acinar cells expressed mCherry as the concentration of dox was lowered. Indeed, a 10-fold lower concentration of dox to induced 3TF expression

resulted in over a 60% reduction in the number of acinar cells expressing 3TF after 1 day of dox (78 ± 2.5% vs. 30 ± 9.9%; n=3). In addition, after 7 days of dox treatment, the pancreas in both groups was nearly normal in size (Figure 4A), cytokeratin staining was either reduced or absent (Figure S6A, B), and CD45 staining was reduced (Figure 4C, D). Most importantly, mice treated with the 10-fold lower concentration of dox (0.2 mg/ml) exhibited many mCherry$^+$ cells that co-expressed low levels of insulin (Figure 4E, F). On the other hand, mice given the lowest concentration of dox (0.02 mg/ml) had no mCherry$^+$/insulin$^+$ co-expressing cells nor any mCherry$^+$ cells that co-expressed chromogranin A or ghrelin (Figure S6C–F). Instead, the mCherry$^+$ cells in these animals continued to express amylase at 7 days (Figure S6G–H), indicating that they had undergone very little, if any, A→β reprogramming within the one week experimental timeframe. Taken together, these findings indicate that A→β reprogramming depends on the magnitude of 3TF expression. When it is too low, no reprogramming occurs. Conversely, when it is too high, a potent inflammatory response occurs which diverts the reprogramming outcome to an ADM-like phenotype.

Macrophage depletion permits A→β reprogramming

We next sought to determine whether the inflammatory response might be responsible for the divergent reprogramming outcome. Since the majority of immune cells present after 7 days of 3TF expression were macrophages, we administered gadolinium chloride ($GdCl_3$), a macrophage toxin (Jankov et al., 2001), both prior to and during dox treatment. The depletion of macrophages in the pancreas was confirmed by immunostaining for F4/80 (Figure 5A, B). Strikingly, the pancreata of mice treated with $GdCl_3$ were nearly normal in both size and appearance (Figure 5C, D). Animals administered $GdCl_3$ did not exhibit either the formation of tubular complexes or the diffuse cytokeratin-staining that characterized the diallelic mice not administered $GdCl_3$ (Figure 5E–G and 6A) nor did they exhibit fibrosis (Figure 6B). More importantly, approximately 6% of the mCherry$^+$ cells present after 7 days of dox treatment co-expressed insulin (Figure 6C, D). Cell counting after 7 days of treatment revealed approximately 650,000 new β-like cells per animal (Table S5). Interestingly cell counting also revealed a decrease in the number of cells expressing mCherry at 7 days of dox.

To further confirm that macrophage depletion promotes 3TF-mediated A→β reprogramming, RT-qPCR was performed on FACS-sorted mCherry$^+$ cells. Indeed, both *Ins1* and *Ins2* mRNA were increased after 7 days of dox in mice administered $GdCl_3$ (Figure 6E). Contrary to immunofluorescence analysis, RT-qPCR also revealed a modest increase in *Ins1* and *Ins2* mRNA in FACS-sorted mCherry$^+$ cells from mice that were only administered dox (Figure 6E). These discordant findings suggest that dox-only treated mice may produce *Ins1* and *Ins2* mRNA but not insulin protein, perhaps due to the inflammation, ER stress, and activation of the UPR, which is known to impair protein translation. These findings suggest that the overly robust expression of 3TF triggers a potent inflammatory response, mediated by macrophages, that prevents A→β reprogramming.

To assess the function of the newly generated β-like cells, mice were rendered diabetic by administration of the β-cell toxin streptozotocin (STZ), treated with $GdCl_3$ to attenuate inflammation, then robust 3TF expression was induced with 2 mg/ml dox. Within two days

of dox treatment, the diabetic mice began to exhibit an improvement in blood glucose concentration, and at 6 days, their blood glucose concentrations were indistinguishable from untreated control animals (Figure 7A). Furthermore, by day 7 of dox, two mice died with low blood glucose levels (86 and 72 mg/dl). Removal of dox at day 7 was followed immediately by a worsening of glycemic control and reversion to a diabetic state within a few days. Interestingly, intraperitoneal glucose tolerance tests (GTT) performed after 7 days of dox treatment revealed two different patterns of response in the five mice treated. Two mice appeared to be glucose responsive whereas the other three mice, which were hypoglycemic at the beginning of GTT, lacked glucose-sensitive insulin secrection (Figure 7B). In any case, these findings indicate a sufficient number of new β-like cells were produced to rescue STZ-induced diabetes and that the production of insulin by these cells was dox-dependent. In addition, our results suggest the presence of at least two subgroups of reprogrammed β-like cells, one group that is glucose responsive and a second that may constitutively secrete insulin in a non-glucose responsive manner.

Finally, we sought to determine whether the efficiency of 3TF-mediated A→β reprogramming could be increased by simultaneously lowering the concentration of dox and attenuating inflammation by depleting macrophages. Interestingly, while the dual treatment very clearly preserved pancreatic mass and histology (Figure S7A–C), prevented abnormal cytokeratin staining (Figure S7D–F), and further decreased tissue inflammation (Figure S7G–I), it did not increase the overall reprogramming efficiency (Figure S7J, K).

Discussion

Our findings indicate that the overly robust expression of 3TF in acinar cells induces pancreatic inflammation which blocks A→β reprogramming and results, instead, in the production of new duct-like cells (Figure 7C). Only when inflammation is attenuated, either by reducing the intensity of 3TF expression or by depleting macrophages, does the production of new β-like cells occur. We suggest that when the concentration of 3TF is too high, pancreatic acinar cell stress and damage occurs thereby causing cytokine release, macrophage infiltration, and ADM, which prevents A→β reprogramming. We further suggest that efficient reprogramming requires a coordinated series of events whereby acinar cells cease zymogen production, delaminate and migrate to the surrounding mesenchyme, then cluster into new vascularized islets. For these cellular changes to occur without causing cellular damage and inducing inflammation, acinar cells may need time to cease the production and secretion of tissue-digesting enzymes before delamination from the pancreatic duct.

The pace at which reprogramming occurs is likely influenced by the concentration of the reprogramming factors. If 3TF expression is too high, and reprogramming occurs at a rate that exceeds the ability of the cell to undergo an orderly transition from one cell state (acinar) to another (endocrine), acinar cell damage may occur, preventing the formation of new β-like cells. Indeed, when we reduced the level of 3TF expression, the inflammatory response was attenuated and new β-like cells were produced. Conversely, if 3TF levels are too low, no reprogramming occurs, at least within a one week timeframe. Such a conclusion

is consistent with previous studies that have shown the importance of factor levels in achieving successful reprogramming (Carey et al., 2011; Tonge et al., 2014).

We also found that the presence of inflammatory macrophages within the pancreas greatly influences the outcome of 3TF-mediated acinar cell reprogramming. While depleting either T- or B-cells during reprogramming does not prevent ADM or allow for the production of new β-like cells, the depletion of macrophages, by the administration of $GdCl_3$, prevented ADM, thereby enabling acinar cells to be reprogrammed into β-like cells. The mechanisms involved in the macrophage-dependent blockage of A→β reprogramming remain unclear, but it has been reported that macrophage-secreted cytokines mediate ADM through activation of NFκB and STAT3 (Liou et al., 2013). While our RNA-Seq data suggest that inflammation enhances signaling through NFκB, STAT3 signaling was recently shown to be required for cytokine-mediated A→β conversion (Baeyens et al., 2013). Thus, it is possible that NFκB and STAT3 signaling oppose each other, with STAT3 signaling promoting A→β reprogramming and NFκB signaling impairing reprogramming by causing ADM.

We estimate that approximately 650,000 new β-like cells are produced, on average, in response to administration of 2 mg/ml dox and $GdCl_3$. While this number of cells is about a third of the approximately 2 million β-cells in an average mouse pancreas (Dor et al., 2004), it is sufficient to transiently rescue STZ-induced diabetes. However, the ability of these new β-like cells to stably secrete insulin in a glucose-dependent manner is not established after only 6 days of 3TF treatment since the removal of dox at 7 days caused a quick reversion to a diabetic state. These findings are consistent with prior studies that used adenoviral delivery of the same three transcription factors in which two months were required for the reprogrammed acinar cells to adopt a DNA methylation and transcriptional profile similar to that of endogenous β-cells (Li et al., 2014b). Thus, our findings support the notion that an extended exposure to the three reprogramming factors is necessary for acinar cells to adopt both the epigenetic and transcriptional profile of an endogenous β-cell.

Adenoviral delivery of the reprogramming factors has been reported to result in 40–50% of infected acinar cells being converted to new β-like cells (Li et al., 2014b). While we expected that the transgenic delivery of the factors would further improve reprogramming efficiency, we found the opposite with only 6% of 3TF-expressing cells expressing insulin after 7 days. This suggests that there are additional variables that distinguish adenoviral- and transgene-mediated reprogramming, such as the dynamics of 3TF-expression. While use of the Tet-On system has the distinct advantage of allowing us to simultaneously control the concentration and duration of 3TF expression, it does not allow stable expression of the reprogramming factors over an extended time. Use of the *Ptf1a* gene to drive expression of rtTA, while being a straightforward means of achieving acinar-cell specificity, has the limitation that *Ptf1a* expression is extinguished as acinar cells are converted into new β-cells. This limitation can only be overcome with a more complicated transgene design.

Widespread metaplastic changes resulting from tissue inflammation have not been reported when adenoviruses are used to introduce the reprogramming factors into the pancreas of normoglycemic mice (Cavelti-Weder et al., 2016). We speculate that similar metaplastic conversions are not observed due to the low infection efficiency of the adenovirus, which

results in fewer acinar cells expressing the reprogramming factors, thereby avoiding triggering widespread pancreatic inflammation and allowing for more of the virally-infected cells to be reprogrammed. However, despite the highly penetrant expression of 3TF in our transgene-based model (nearly 80% of acinar cells at 2 mg/ml dox), we could only achieve the visible reprogramming of 6% of the 3TF-induced cells. Even so, we were able to produce over twice the number of new insulin-positive cells (650,000 versus 245,000 ± 32,000) that were reported when using an adenovirus (Li et al., 2014c). This very marked difference in experimental outcome is likely due to our inability to fully suppress pancreatic inflammation when using a high dose of dox to express 3TF in the maximum number of acinar cells.

In any case, the very marked differences in our experimental outcomes compared to those achieved using an adenovirus suggest that both the dynamics and secondary effects of A→β reprogramming are complex. However, by exploring the outcomes achieved with a transgene-based reprogramming model, we have obtained a better understanding of some of the many variables that will need to be understood to be able to safely and efficiently reprogram acinar cells in humans.

Experimental Procedures

Mouse lines and husbandry

All animals were housed at Vanderbilt Institutional Animal Care Facility and experimental protocols were approved by Vanderbilt Institutional Animal Care and Use Committee. Mice were treated with doxycycline (dox) (Sigma) dissolved in a 5% sucrose solution beginning at 6 to 8 weeks of age. Dox was provided *ad libitum* in lieu of the normal water supply. *Rag1*$^{-/-}$ mice (Mombaerts et al., 1992) were purchased from Jackson Laboratory. *Ptf1a*$^{YFP/+}$ (Burlison et al., 2008) and *MIP.GFP* mice (Hara et al., 2003) were genotyped as previously described. Generation of new mouse alleles and validation methods are described in Supplemental Information.

Microscopy

mCherry fluorescence intensity measurements in unfixed tissues were performed using a Leica MZ16 FA stereoscope at an exposure time of 39.5 milliseconds. For paraffin sections, pancreatic tissue was fixed with 20% formaldehyde and processed by the Vanderbilt Tissue Pathology Shared Resource (TPSR). H&E, Masson's Trichrome Blue, CD3, F4/80, and Cytokeratin staining was performed by TPSR according to manufacturer's directions. Immunofluorescence staining of frozen sections was performed as previously described (Burlison et al., 2008). See Supplemental Information for a complete list of antibodies. Images were acquired using a Zeiss Axioplan-II upright microscope or a LSM 710 META inverted confocal microscope then pseudo-colored using either ImageJ (NIH) or Zeiss LSM browser software. All images are representative of phenotypes observed in at least three different animals.

Adenovirus construction and injection

The AdV-CMV-3TF virus was made using pAd/CMV/V5-DEST (Invitrogen). High titer virus (6.5×10^{10} plaque-forming units (pfu)) was obtained by purification (Vector biolabs). Mice were subjected to laparotomy under general anesthesia (Ketamine/Xylazine). The splenic lobe of the dorsal pancreas of 8 week old *Rag1*$^{-/-}$ mice was injected with 100 μl of purified AdV-CMV-3TF (2×10^{10} pfu) and AdV-CMV-GFP (1×10^{9} pfu) (Vector Biolabs) and animals were euthanized 7 days later.

Macrophage depletion

6–8 week old mice were intravenously injected with either saline (control) or gadolinium chloride ($GdCl_3$) (10 mg/kg, every 2 days for 1 week prior to dox treatment and then every 3rd day during dox treatment) and administered dox (2.0 or 0.2 mg/ml). Pancreata were harvested 7 days after dox. Only animals in which macrophages were reduced to less than 15% of the total DAPI-stained cells were used in the study.

Physiological studies

Adult mice were rendered diabetic with a single intraperitoneal injection of streptozotocin (180 mg per kg body weight dissolved in citrate buffer (pH 4.5)) after 4 hours fast. Mice with blood glucose levels >300 mg/dL were used for experiments. Glucose tolerance tests were performed by fasting animals overnight (16-hours) followed by an intraperitoneal injection of D-glucose (2 g per kg body weight). Blood glucose concentrations were measured using a BD Logic glucometer.

RT-qPCR analysis

cDNA was prepared from RNA using a high-capacity cDNA Archive Kit (Life Technologies) and amplified using real-time PCR with Power SYBR Green PCR master mix (Life Technologies) using gene specific primers (Table S6). Three experimental RNA replicates for each genotype were assayed. PCR was performed with an ABI 7900HT real-time PCR system (Life Technologies) and amplification data was analyzed using Sequence Detection System version 2.1 (Life Technologies) and Excel software (Microsoft). *Hprt* was used as an endogenous control for normalization and comparative C_t method was used to calculate relative fold expression by $2^{-\Delta\,\Delta Ct}$.

RNA-seq Analysis

Three independent RNA isolates from each genotype were used for sequencing. RNA-sequencing methods were described previously (Choi et al., 2012). Single-end sequencing (110 bp) was performed on Illumina HiSeq2000 genome analyzer. Read alignment to the mouse genome (mm10) was performed using RNA-Seq Unified Mapper (RUM) (Grant et al., 2011). Genome alignment of sequencing data yielded 32–84 million uniquely mapped reads. Data was pre-processed with the PORT pipeline (https://github.com/itmat/Normalization; Kim *et al.* manuscript in preparation). Functional Annotation Clustering was performed using DAVID Bioinformatics Resources v.6.7 (Huang da et al., 2009). See Supplemental Information for detailed information on RNA isolation and preprocessing and differential expression analyses.

Quantification of necrosis

Necrosis in pancreatic acini was conducted as previously described (Liu et al., 2014; Yuan et al., 2012).

Cell quantification

Cells co-expressing specific genes was determined by manual counting. For each animal, over 500 cells were counted using ImageJ from five sections per animal that were separated by approximately 50 μM. All key experimental findings were observed in 3 or more animals. The total number of cells in the adult mouse pancreas was previously calculated (Dore et al., 1981) and used to determine the number of new β-cells produced.

Statistical methods

Statistical difference between two groups was assessed using student's t-tests. *$p < 0.05$, **$p < 0.001$. All data represent mean ± SEM.

Supplementary Material

Refer to Web version on PubMed Central for supplementary material.

Acknowledgments

These studies were supported by NIH grants DK72473 and DK89523 to MAM. We thank Haibo Jia for helping derive the *Ptf1a*^{rtTA} allele, Lori Sussel, Ray MacDonald, Chris Wright, and Roland Stein for helpful suggestions or reagents, Jody Peters, Rama Gangula, and Laurel Grower for their skilled assistance with mouse husbandry, surgery, adenoviral construction, and genotyping, and Tiziana Sanavia for initial QC on the RNA-seq datasets. We thank the staff of the Vanderbilt Transgenic/ESC Shared Resource, Flow Cytometry Core, Translational Pathology Shared Resource, and VANTAGE for their help in deriving mice, staining slides, sorting cells, and performing RNA-Seq. The authors declare no conflict of interest.

References

Arnes L, Hill JT, Gross S, Magnuson MA, Sussel L. Ghrelin expression in the mouse pancreas defines a unique multipotent progenitor population. PLoS One. 2012; 7:e52026. [PubMed: 23251675]

Baeyens L, Lemper M, Leuckx G, De Groef S, Bonfanti P, Stange G, Shemer R, Nord C, Scheel DW, Pan FC, et al. Transient cytokine treatment induces acinar cell reprogramming and regenerates functional beta cell mass in diabetic mice. Nat Biotechnol. 2013

Bockman DE, Muller M, Buchler M, Friess H, Beger HG. Pathological changes in pancreatic ducts from patients with chronic pancreatitis. Int J Pancreatol. 1997; 21:119–126. [PubMed: 9209953]

Bramswig NC, Everett LJ, Schug J, Dorrell C, Liu C, Luo Y, Streeter PR, Naji A, Grompe M, Kaestner KH. Epigenomic plasticity enables human pancreatic alpha to beta cell reprogramming. J Clin Invest. 2013; 123:1275–1284. [PubMed: 23434589]

Burlison JS, Long Q, Fujitani Y, Wright CV, Magnuson MA. Pdx-1 and Ptf1a concurrently determine fate specification of pancreatic multipotent progenitor cells. Dev Biol. 2008; 316:74–86. [PubMed: 18294628]

Carey BW, Markoulaki S, Hanna JH, Faddah DA, Buganim Y, Kim J, Ganz K, Steine EJ, Cassady JP, Creyghton MP, et al. Reprogramming factor stoichiometry influences the epigenetic state and biological properties of induced pluripotent stem cells. Cell Stem Cell. 2011; 9:588–598. [PubMed: 22136932]

Cavelti-Weder C, Li W, Zumsteg A, Stemann-Andersen M, Zhang Y, Yamada T, Wang M, Lu J, Jermendy A, Bee YM, et al. Hyperglycaemia attenuates in vivo reprogramming of pancreatic exocrine cells to beta cells in mice. Diabetologia. 2016; 59:522–532. [PubMed: 26693711]

Chen SX, Osipovich AB, Ustione A, Potter LA, Hipkens S, Gangula R, Yuan W, Piston DW, Magnuson MA. Quantification of factors influencing fluorescent protein expression using RMCE to generate an allelic series in the ROSA26 locus in mice. Dis Model Mech. 2011; 4:537–547. [PubMed: 21324933]

Choi E, Kraus MR, Lemaire LA, Yoshimoto M, Vemula S, Potter LA, Manduchi E, Stoeckert CJ Jr, Grapin-Botton A, Magnuson MA. Dual lineage-specific expression of Sox17 during mouse embryogenesis. Stem Cells. 2012; 30:2297–2308. [PubMed: 22865702]

Dor Y, Brown J, Martinez OI, Melton DA. Adult pancreatic beta-cells are formed by self-duplication rather than stem-cell differentiation. Nature. 2004; 429:41–46. [PubMed: 15129273]

Dore BA, Grogan WM, Madge GE, Webb SR. Biphasic development of the postnatal mouse pancreas. Biol Neonate. 1981; 40:209–217. [PubMed: 7032613]

Grant GR, Farkas MH, Pizarro AD, Lahens NF, Schug J, Brunk BP, Stoeckert CJ, Hogenesch JB, Pierce EA. Comparative analysis of RNA-Seq alignment algorithms and the RNA-Seq unified mapper (RUM). Bioinformatics. 2011; 27:2518–2528. [PubMed: 21775302]

Gu G, Dubauskaite J, Melton DA. Direct evidence for the pancreatic lineage: NGN3+ cells are islet progenitors and are distinct from duct progenitors. Development. 2002; 129:2447–2457. [PubMed: 11973276]

Halangk W, Lerch MM, Brandt-Nedelev B, Roth W, Ruthenbuerger M, Reinheckel T, Domschke W, Lippert H, Peters C, Deussing J. Role of cathepsin B in intracellular trypsinogen activation and the onset of acute pancreatitis. J Clin Invest. 2000; 106:773–781. [PubMed: 10995788]

Hara M, Wang X, Kawamura T, Bindokas VP, Dizon RF, Alcoser SY, Magnuson MA, Bell GI. Transgenic mice with green fluorescent protein-labeled pancreatic beta-cells. Am J Physiol Endocrinol Metab. 2003; 284:E177–183. [PubMed: 12388130]

Huang da W, Sherman BT, Lempicki RA. Systematic and integrative analysis of large gene lists using DAVID bioinformatics resources. Nat Protoc. 2009; 4:44–57. [PubMed: 19131956]

Huang HP, Liu M, El-Hodiri HM, Chu K, Jamrich M, Tsai MJ. Regulation of the pancreatic islet-specific gene BETA2 (neuroD) by neurogenin 3. Mol Cell Biol. 2000; 20:3292–3307. [PubMed: 10757813]

Jankov RP, Luo X, Belcastro R, Copland I, Frndova H, Lye SJ, Hoidal JR, Post M, Tanswell AK. Gadolinium chloride inhibits pulmonary macrophage influx and prevents O(2)-induced pulmonary hypertension in the neonatal rat. Pediatr Res. 2001; 50:172–183. [PubMed: 11477200]

Ji B, Chen XQ, Misek DE, Kuick R, Hanash S, Ernst S, Najarian R, Logsdon CD. Pancreatic gene expression during the initiation of acute pancreatitis: identification of EGR-1 as a key regulator. Physiol Genomics. 2003; 14:59–72. [PubMed: 12709512]

Jura N, Archer H, Bar-Sagi D. Chronic pancreatitis, pancreatic adenocarcinoma and the black box in-between. Cell Res. 2005; 15:72–77. [PubMed: 15686632]

Khoo C, Yang J, Weinrott SA, Kaestner KH, Naji A, Schug J, Stoffers DA. Research resource: the pdx1 cistrome of pancreatic islets. Mol Endocrinol. 2012; 26:521–533. [PubMed: 22322596]

Lee J, Sayed N, Hunter A, Au KF, Wong WH, Mocarski ES, Pera RR, Yakubov E, Cooke JP. Activation of innate immunity is required for efficient nuclear reprogramming. Cell. 2012; 151:547–558. [PubMed: 23101625]

Li J, Zhou R, Zhang J, Li ZF. Calcium signaling of pancreatic acinar cells in the pathogenesis of pancreatitis. World J Gastroenterol. 2014a; 20:16146–16152. [PubMed: 25473167]

Li W, Cavelti-Weder C, Zhang Y, Clement K, Donovan S, Gonzalez G, Zhu J, Stemann M, Xu K, Hashimoto T, et al. Long-term persistence and development of induced pancreatic beta cells generated by lineage conversion of acinar cells. Nat Biotechnol. 2014b; 32:1223–1230. [PubMed: 25402613]

Li W, Nakanishi M, Zumsteg A, Shear M, Wright C, Melton DA, Zhou Q. In vivo reprogramming of pancreatic acinar cells to three islet endocrine subtypes. Elife. 2014c; 3:e01846. [PubMed: 24714494]

Liou GY, Doppler H, Necela B, Krishna M, Crawford HC, Raimondo M, Storz P. Macrophage-secreted cytokines drive pancreatic acinar-to-ductal metaplasia through NF-kappaB and MMPs. J Cell Biol. 2013; 202:563–577. [PubMed: 23918941]

Liu Y, Yuan J, Tan T, Jia W, Lugea A, Mareninova O, Waldron RT, Pandol SJ. Genetic inhibition of protein kinase Cepsilon attenuates necrosis in experimental pancreatitis. Am J Physiol Gastrointest Liver Physiol. 2014; 307:G550–563. [PubMed: 25035113]

Logsdon CD, Ji B. The role of protein synthesis and digestive enzymes in acinar cell injury. Nat Rev Gastroenterol Hepatol. 2013; 10:362–370. [PubMed: 23507798]

Mombaerts P, Iacomini J, Johnson RS, Herrup K, Tonegawa S, Papaioannou VE. RAG-1-deficient mice have no mature B and T lymphocytes. Cell. 1992; 68:869–877. [PubMed: 1547488]

Neurath H, Walsh KA. Role of proteolytic enzymes in biological regulation (a review). Proc Natl Acad Sci U S A. 1976; 73:3825–3832. [PubMed: 1069267]

Pan FC, Bankaitis ED, Boyer D, Xu X, Van de Casteele M, Magnuson MA, Heimberg H, Wright CV. Spatiotemporal patterns of multipotentiality in Ptf1a-expressing cells during pancreas organogenesis and injury-induced facultative restoration. Development. 2013; 140:751–764. [PubMed: 23325761]

Parsa I, Longnecker DS, Scarpelli DG, Pour P, Reddy JK, Lefkowitz M. Ductal metaplasia of human exocrine pancreas and its association with carcinoma. Cancer Res. 1985; 45:1285–1290. [PubMed: 2982487]

Puri S, Folias AE, Hebrok M. Plasticity and dedifferentiation within the pancreas: development, homeostasis, and disease. Cell Stem Cell. 2015; 16:18–31. [PubMed: 25465113]

Rooman I, Real FX. Pancreatic ductal adenocarcinoma and acinar cells: a matter of differentiation and development? Gut. 2012; 61:449–458. [PubMed: 21730103]

Sah RP, Garg SK, Dixit AK, Dudeja V, Dawra RK, Saluja AK. Endoplasmic reticulum stress is chronically activated in chronic pancreatitis. J Biol Chem. 2014; 289:27551–27561. [PubMed: 25077966]

Smith SB, Gasa R, Watada H, Wang J, Griffen SC, German MS. Neurogenin3 and hepatic nuclear factor 1 cooperate in activating pancreatic expression of Pax4. J Biol Chem. 2003; 278:38254–38259. [PubMed: 12837760]

Strobel O, Dor Y, Alsina J, Stirman A, Lauwers G, Trainor A, Castillo CF, Warshaw AL, Thayer SP. In vivo lineage tracing defines the role of acinar-to-ductal transdifferentiation in inflammatory ductal metaplasia. Gastroenterology. 2007; 133:1999–2009. [PubMed: 18054571]

Szilagyi L, Kenesi E, Katona G, Kaslik G, Juhasz G, Graf L. Comparative in vitro studies on native and recombinant human cationic trypsins. Cathepsin B is a possible pathological activator of trypsinogen in pancreatitis. J Biol Chem. 2001; 276:24574–24580. [PubMed: 11312265]

Thorel F, Nepote V, Avril I, Kohno K, Desgraz R, Chera S, Herrera PL. Conversion of adult pancreatic alpha-cells to beta-cells after extreme beta-cell loss. Nature. 2010; 464:1149–1154. [PubMed: 20364121]

Tonge PD, Corso AJ, Monetti C, Hussein SM, Puri MC, Michael IP, Li M, Lee DS, Mar JC, Cloonan N, et al. Divergent reprogramming routes lead to alternative stem-cell states. Nature. 2014; 516:192–197. [PubMed: 25503232]

Van Acker GJ, Saluja AK, Bhagat L, Singh VP, Song AM, Steer ML. Cathepsin B inhibition prevents trypsinogen activation and reduces pancreatitis severity. Am J Physiol Gastrointest Liver Physiol. 2002; 283:G794–800. [PubMed: 12181196]

Wang AY, Ehrhardt A, Xu H, Kay MA. Adenovirus transduction is required for the correction of diabetes using Pdx-1 or Neurogenin-3 in the liver. Mol Ther. 2007; 15:255–263. [PubMed: 17235302]

Wang RN, Kloppel G, Bouwens L. Duct- to islet-cell differentiation and islet growth in the pancreas of duct-ligated adult rats. Diabetologia. 1995; 38:1405–1411. [PubMed: 8786013]

Watada H, Kajimoto Y, Umayahara Y, Matsuoka T, Kaneto H, Fujitani Y, Kamada T, Kawamori R, Yamasaki Y. The human glucokinase gene beta-cell-type promoter: an essential role of insulin promoter factor 1/PDX-1 in its activation in HIT-T15 cells. Diabetes. 1996; 45:1478–1488. [PubMed: 8866550]

Watada H, Scheel DW, Leung J, German MS. Distinct gene expression programs function in progenitor and mature islet cells. J Biol Chem. 2003; 278:17130–17140. [PubMed: 12604598]

Whitcomb DC, Gorry MC, Preston RA, Furey W, Sossenheimer MJ, Ulrich CD, Martin SP, Gates LK Jr, Amann ST, Toskes PP, et al. Hereditary pancreatitis is caused by a mutation in the cationic trypsinogen gene. Nat Genet. 1996; 14:141–145. [PubMed: 8841182]

Yuan J, Liu Y, Tan T, Guha S, Gukovsky I, Gukovskaya A, Pandol SJ. Protein kinase d regulates cell death pathways in experimental pancreatitis. Front Physiol. 2012; 3:60. [PubMed: 22470346]

Zaldumbide A, Carlotti F, Goncalves MA, Knaan-Shanzer S, Cramer SJ, Roep BO, Wiertz EJ, Hoeben RC. Adenoviral vectors stimulate glucagon transcription in human mesenchymal stem cells expressing pancreatic transcription factors. PLoS One. 2012; 7:e48093. [PubMed: 23110179]

Zhou Q, Brown J, Kanarek A, Rajagopal J, Melton DA. In vivo reprogramming of adult pancreatic exocrine cells to beta-cells. Nature. 2008; 455:627–632. [PubMed: 18754011]

Ziv O, Glaser B, Dor Y. The plastic pancreas. Dev Cell. 2013; 26:3–7. [PubMed: 23867225]

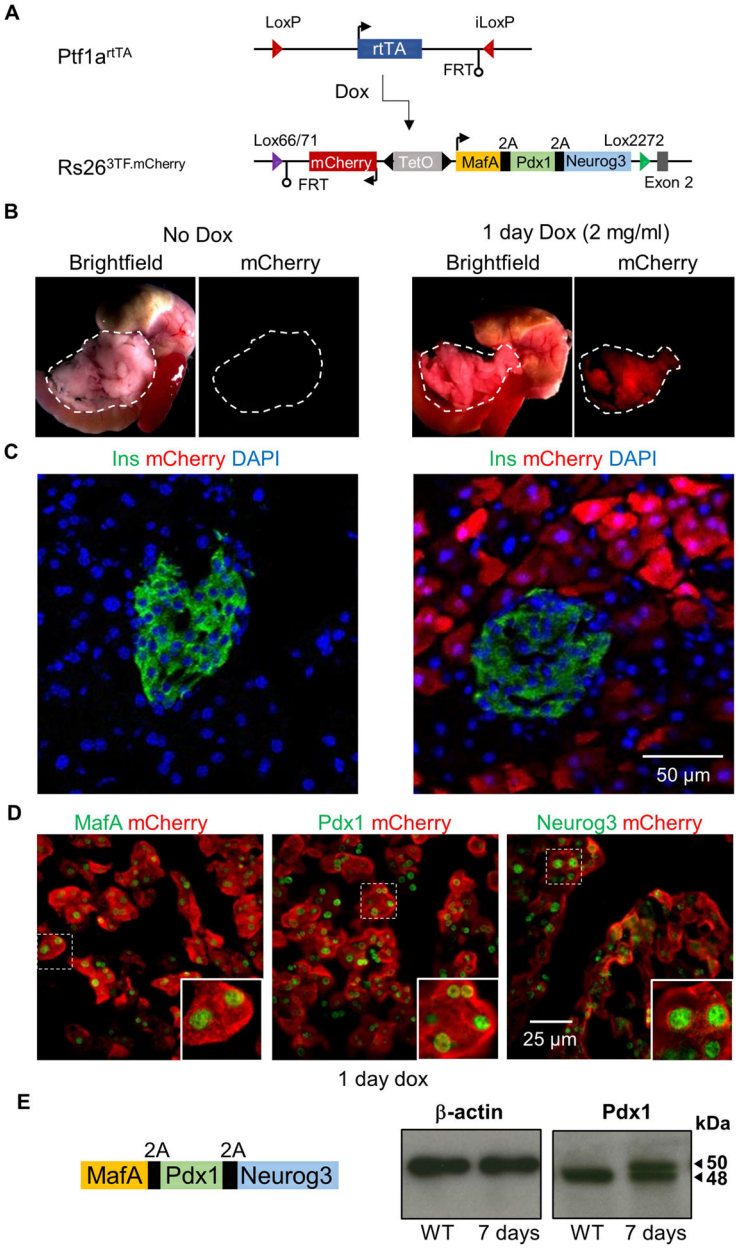

Figure 1. Design and validation of mouse alleles for the dox-dependent expression of 3TF in pancreatic acinar cells

(A) *Ptf1a*^{rtTA} and *Rosa26*$^{3TF.mCherry}$ alleles were generated by recombinase-mediated cassette exchange. When interbred, the two alleles result in dox-inducible expression of *MafA, Pdx1*, *Neurog3,* and mCherry in a pancreatic acinar cell-specific manner. (B) mCherry expression was visible after administering 2.0 mg/ml of dox for 1 day (n=5). mCherry fluorescence was restricted to the pancreas (outlined) of dox treated mice and was not observed in other tissues. (C) Dox-inducible, acinar cell-specific expression of mCherry was confirmed with immunofluorescence analysis. Pancreas sections stained with insulin and mCherry showed that the two proteins were not co-localized. (D) Pancreas sections

stained with antibodies against mCherry and either *MafA, Pdx1*, or *Neurog3* showed co-expression of mCherry and 3TF after 1 day of dox. (E) Schematic of the transgene showing that the protein sequences for MAFA and NEUROG3 flank PDX1. To determine whether proper 2A mediated cleavage of 3TF was achieved, western blot against PDX1 was performed on pancreatic lysate from wild-type (WT) and 7 day induced, $Ptf1a^{rtTA/+}$; $Rosa26^{3TF.mCherry/+}$ (3TF) mice. Arrows indicate both the 50 kDa PDX1 protein with the addition of the 2A peptide sequences and the endogenous PDX1 at 48 kDa. See also Figures S1 and Table S6.

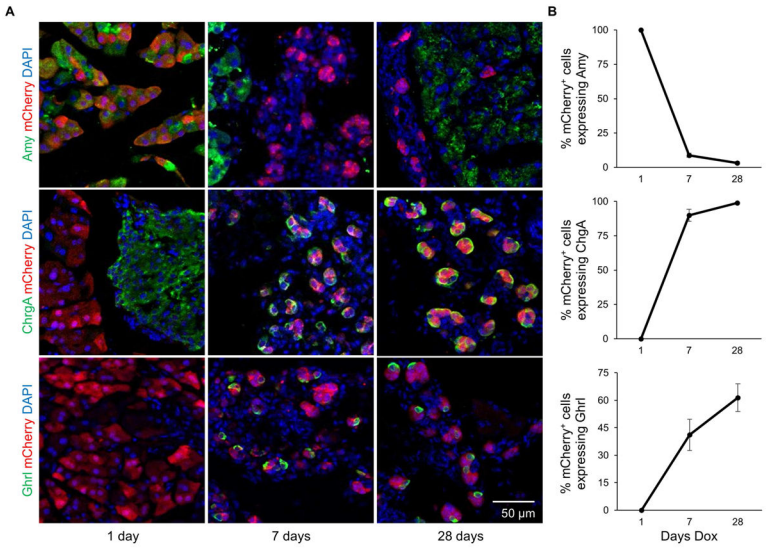

Figure 2. Temporal effects of 3TF overexpression in acinar cells

(A) Animals were induced for 1, 7, or 28 days with dox. Immunofluorescence analysis revealed that amylase expression in mCherry^{+} cells decreased by 7 days and continued to decrease throughout the time course. Simultaneously, expression of chromogranin A and ghrelin began at 7 days and increased during the time-course. (B) Percentage of cells expressing amylase, chromogranin A and ghrelin among mCherry^{+} cells. Three mice per time point. Over 500 mCherry^{+} cells counted for each mouse. Data are represented as mean ± SEM. See also Figure S2 and Table S1–3.

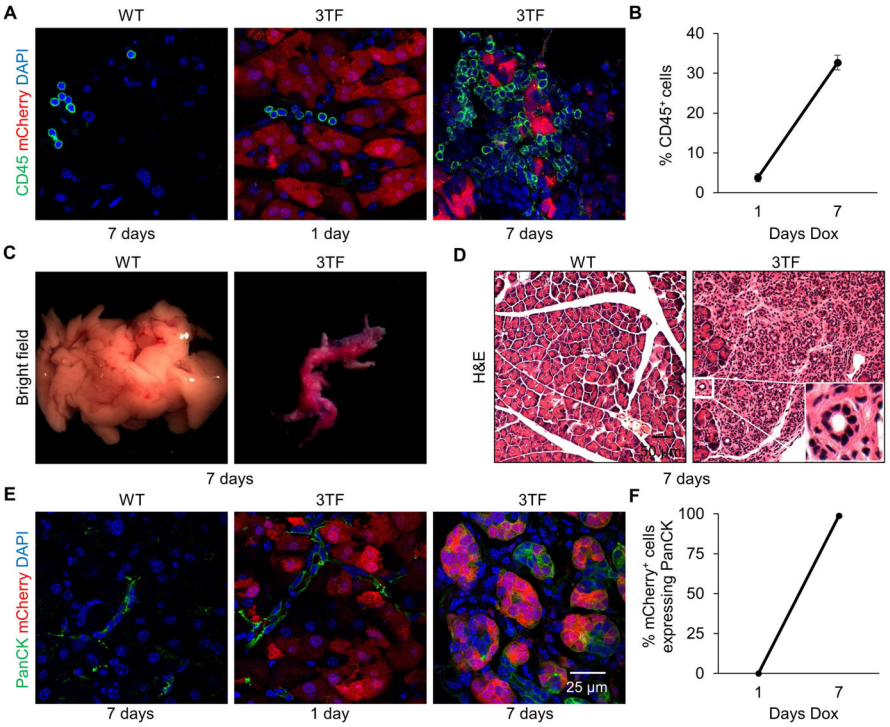

Figure 3. Transgene-mediated 3TF expression in pancreatic acinar cells causes a potent inflammatory response and ADM

(A) Pancreatic immunofluorescence staining of CD45 from WT mice after 7 days of dox and 3TF mice after 1 and 7 days of dox. (B) Percentage of $CD45^+$ cells among $DAPI^+$ cells. Three mice per time point and over 1,000 $DAPI^+$ cells counted for each mouse. Data are represented as mean ± SEM. (C) Representative pancreata and (D) hematoxylin and eosin (H&E) staining of WT and 3TF mice after 7 days of dox. Pancreas of 3TF mice is characterized by the presence of abundant tubular complexes (inset). (E) Pancreatic immunofluorescence staining of PanCK, a ductal marker, from WT mice after 7 days dox and 3TF mice after 1 and 7 days of dox. (F) Percentage of $PanCK^+$ cells among $mCherry^+$ cells. Three mice per time point and over 500 $mCherry^+$ cells counted for each mouse. Data are represented as mean ± SEM. See also Figures S3–S5 and Table S4.

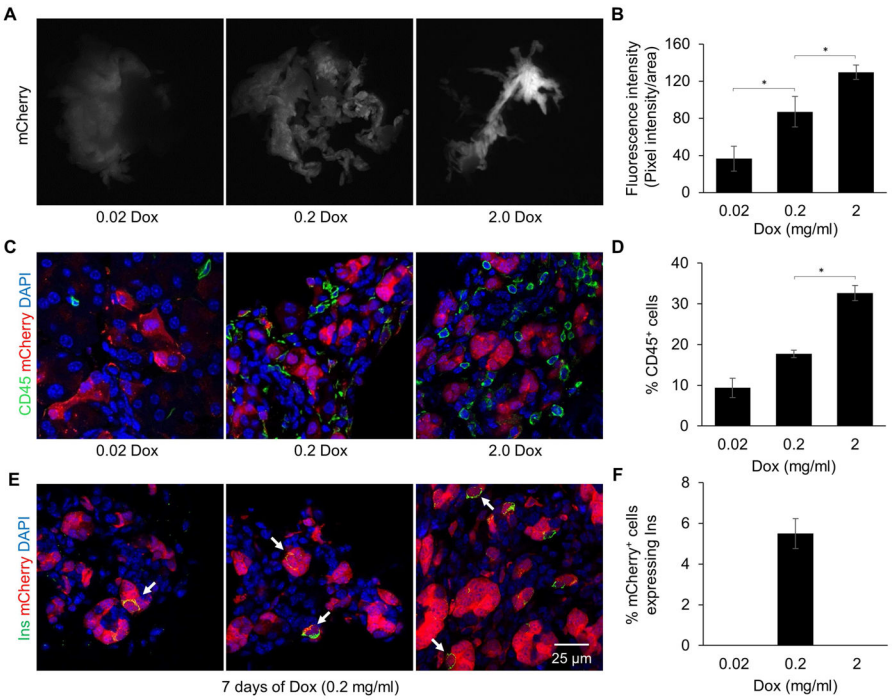

Figure 4. Reducing 3TF expression attenuates inflammation and promotes A→β reprogramming

(A) mCherry fluorescence in the pancreas of 3TF mice administered either 0.02, 0.2, or 2.0 mg/ml of dox for 7 days. (B) Quantification of fluorescence intensity per pancreas area. Data are represented as mean ± SEM. *$p < 0.05$, student's t-test. (C) Pancreatic immunofluorescence CD45 staining of 3TF mice administered varying concentrations of dox at 7 days. (D) Percentage of $CD45^+$ cells among $DAPI^+$ cells. Three mice per time point and over 1,000 $DAPI^+$ cells counted for each mouse. Data are represented as mean ± SEM. *$p < 0.05$, student's t-test (E) Pancreatic immunofluorescence insulin staining of 3TF mice administered 0.2 mg/ml of dox for 7 days. $mCherry^+$ cells that co-expressed insulin (arrows) were observed. (F) Percentage of $insulin^+$ cells among $mCherry^+$ cells. Three mice per time point and over 500 $mCherry^+$ cells counted for each mouse. Data are represented as mean ± SEM. See also Figure S6.

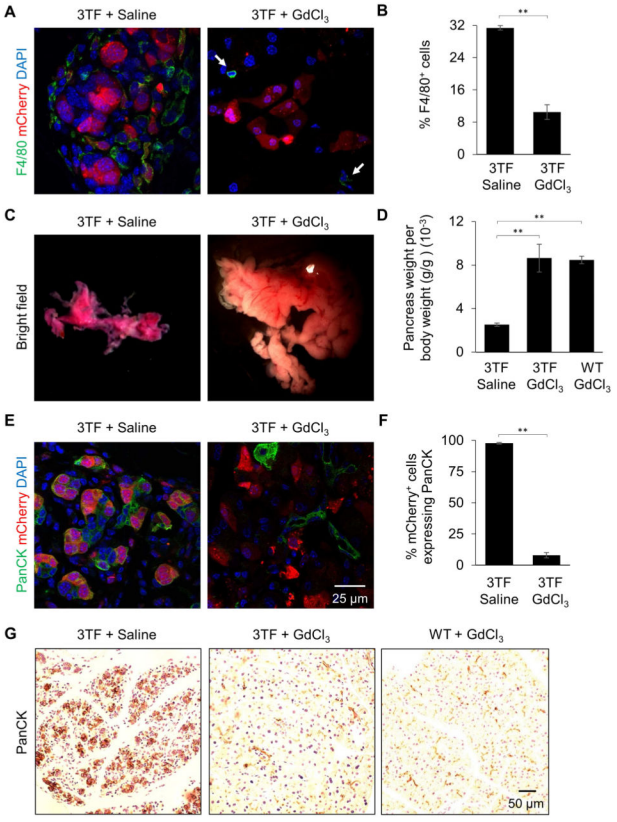

Figure 5. Macrophage depletion preserves pancreatic mass and architecture

(A) Pancreatic immunofluorescence F4/80 staining of 3TF mice administered either saline or $GdCl_3$ after 7 days dox. Arrows indicate $F4/80^+$ cells. (B) Percentage of $F4/80^+$ cells among $DAPI^+$ cells at 7 days dox. Three mice per time point and over 1,000 $DAPI^+$ cells counted for each mouse. Data are represented as mean ± SEM. **$p < 0.001$, student's t-test. (C) Representative pancreata from 3TF mice given either saline or $GdCl_3$ after 7 days dox. (D) Pancreatic weight per body weight of 3TF mice given either saline or $GdCl_3$ and WT mice given $GdCl_3$ after 7 days dox. Data are represented as mean ± SEM. **$p < 0.001$, student's t-test. (E) Pancreatic immunofluorescence staining of PanCK of 3TF mice administered either saline or $GdCl_3$ at 7 days dox. (F) Percentage of $PanCK^+$ cells among $mCherry^+$ cells at 7 days dox. Three mice per time point and over 500 $mCherry^+$ cells counted for each mouse. Data are represented as mean ± SEM. **$p < 0.001$, student's t-test. (G) Pancreatic PanCK staining of 3TF mice administered either saline or $GdCl_3$ and WT mice administered $GdCl_3$ at 7 days dox.

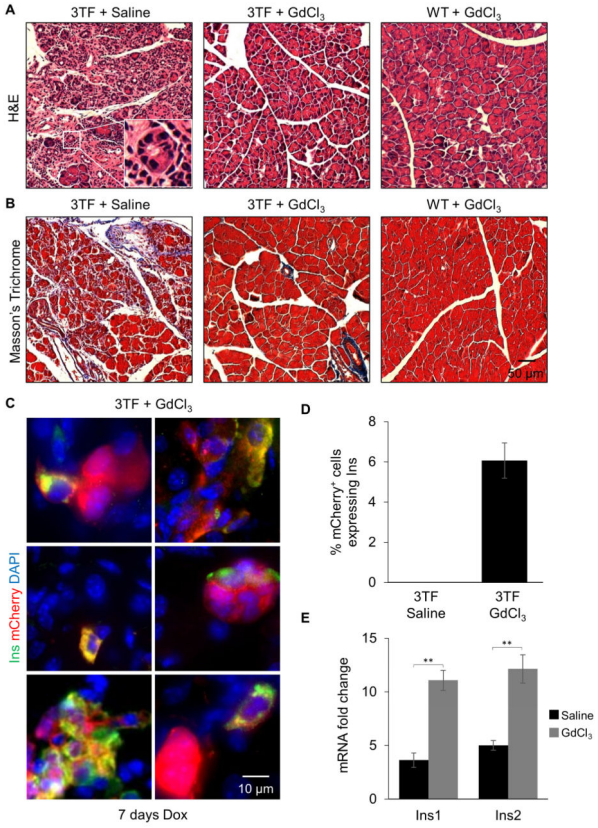

Figure 6. Macrophage depletion promotes A→β reprogramming

(A) Representative H&E staining of 3TF mice administered either saline or $GdCl_3$ and WT mice administered $GdCl_3$ at 7 days dox. Tubular complexes (inset) observed in pancreas of 3TF mice administered saline. (B) Representative Masson's trichrome stain of 3TF mice administered either saline or $GdCl_3$ and WT mice administered $GdCl_3$ at 7 days dox. (C) Pancreatic immunofluorescence insulin staining of 3TF mice administered $GdCl_3$ at 7 days dox. $mCherry^+$ cells that co-expressed insulin were observed. (D) Percentage of $Insulin^+$ cells among $mCherry^+$ cells at 7 days of dox. Three mice per time point and over 1,000 $mCherry^+$ cells counted. Data are represented as mean ± SEM. (E) RT-qPCR analysis of *Ins1* and *Ins2* expression in 3TF mice given either saline or $GdCl_3$ after 7 days of dox. Fold change calculated against mRNA expression in uninduced acinar cells. Data are represented as mean ± SEM. $^{**}p < 0.001$, student's t-test. See also Figure S7 and Table S6.

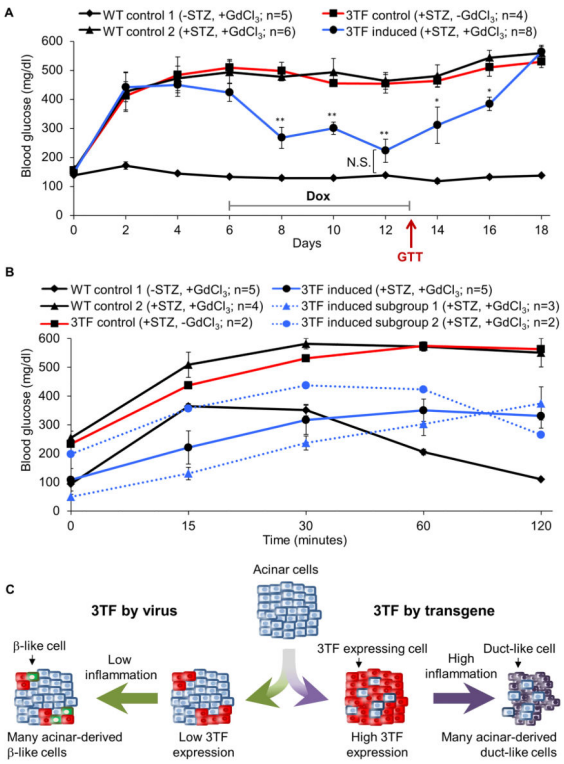

Figure 7. New β-like cells rescue STZ-induced diabetes

(A) Mice were administered STZ on day 0 to induce diabetes and dox was administered for 7 days (day 6–13). Blood glucose was measured every other day. Statisical significance for the 3TF induced group was calculated against the 3TF control group, except were otherwise noted. (B) GTT was performed on day 13. ◆ black line: WT mice administered $GdCl_3$ and dox but not STZ (WT control 1); ▲ black line: WT mice administered STZ, $GdCl_3$, and dox (WT control 2); ■ red line: 3TF mice administered STZ and dox but not $GdCl_3$ (3TF control); ● blue line: 3TF mice administered STZ, $GdCl_3$, and dox (3TF induced). Of the five 3TF induced mice subjected to the GTT, two different patterns of response were observed: mice that were non-glucose responsive (▲ blue dotted line: 3TF induced subgroup 1) and mice that were glucose responsive (● blue dotted line: 3TF induced subgroup 2). (C) Model of divergent 3TF reprogramming. Adenoviral delivery of 3TF to the pancreatic acinar cells of *Rag1*$^{-/-}$ mice is relatively inefficient resulting in only a few pancreatic acinar cells expressing 3TF. Low levels of inflammation permit A→β reprogramming. Transgene expression of 3TF in the pancreatic acinar cells of *Rag1*$^{+/+}$ mice is very efficient resulting in many acinar cells expressing 3TF and high levels of 3TF expression. Rapid reprogramming causes ER stress, a rise in $[Ca^{2+}]_i$, and cell death, triggering a potent inflammatory response that results in ADM, thereby blocking A→β reprogramming. See also Table S5.